Journal of Alloys and Compounds 509 (2011) 7130–7133

Contents lists available at ScienceDirect

Journal of Alloys and Compounds

journal homepage: www.elsevier.com/locate/jallcom

Electrical properties of Li doped sodium potassium niobate thick films prepared by a tape casting process

Fang Fu [a], Bo Shen [a], Jiwei Zhai [a,*], Zhengkui Xu [b], Xi Yao [a]

[a] Functional Materials Research Laboratory, Tongji University, Shanghai 200092, China
[b] Department of Physics and Materials Science, City University of Hong Kong, Hong Kong, PR China

ARTICLE INFO

Article history:
Received 29 December 2010
Received in revised form 1 April 2011
Accepted 1 April 2011
Available online 12 April 2011

Keywords:
Sodium potassium niobate
Thick films
Dielectric response
Piezoelectricity

ABSTRACT

Lithium doped $K_{0.5}Na_{0.5}NbO_3$ (abbreviated as KNN–xL, with $x = 0.02$, 0.04, 0.06, 0.08) thick films with a thickness of about 20 μm were prepared by a tape casting process. The presence of Li ions promoted the microstructure of these thick films. Coercive fields (E_c) of the thick films decreased with the addition of Li ions. Two phase transition temperatures, corresponding to T_{O-T} and T_C, were observed in the KNN–xL thick films. The sample with $x = 0.06$ exhibited an optimized value of d_{33} (91.6 pm/V), which was attributed to the formation of a morphotropic phase boundary.

1. Introduction

Piezoelectric thick films have drawn significant interests in recent years with the development of microelectromechanical systems (MEMS). They are widely used in micropumps, ultrasonic motors, resonators, high-frequency transducers and energy harvesters [1–3]. Thick films offer many advantages over bulk ceramics as components in various electronic devices. Up to now, most thick films used for industrial productions are lead-containing materials, which are harmful to the environment during the fabrication and disposal after usage. More and more studies focused on lead-free materials because of the urgent demands for environmental protection [4,5]. However, the low piezoelectric coefficients of lead-free materials restricted their industrial applications.

Sodium potassium niobate ($K_{0.5}Na_{0.5}NbO_3$ or KNN) is one of the most promising lead-free piezoelectric materials, due to its relatively large piezoelectricity ($d_{33} = 160$ pC/N) and high Curie temperature ($T_C = 420$ °C). Wang et al. [6] fabricated KNN thick films by using a polyvinylpyrrolidone-modified chemical solution deposition method. The thick film had an optimized piezoelectric coefficient of 61 pm/V. Ryu et al. [7] reported a lead-free piezoelectric thick film, $0.948(K_{0.5}Na_{0.5})NbO_3$–$0.052LiSbO_3$, with a piezoelectric coefficient of 50 pm/V, by using an aerosol deposition method. These values are much inferior to that of PZT thick films (60–210 pm/V). It has been shown that compositional modification is one of the effective approaches to improve piezoelectric properties of lead-free materials. Recently, it was found that there is a morphotropic phase boundary (MPB) in KNN ceramics doped with 6% Li [8,9]. The coexistence of tetragonal and orthorhombic phases made polarization more available and thus enhanced the piezoelectric performance of KNN [10,11]. Saito et al. [12] found that textured KNNL ceramics had a piezoelectricity comparable to that of PZT ceramics.

Piezoelectric thick films can be prepared by many techniques, such as screen printing, tape casting, composite sol–gel, electrophoretic deposition, ink-jet printing, and aerosol deposition [13–16]. Tape casting is among the most convenient and economic processes to fabricate thick films. This technique has been widely used for large-scale fabrication of piezoelectric thick films. In the present work, it was used to prepare lithium-doped KNN lead-free thick films. The effect of Li concentration on microstructure and electrical properties of the thick films was investigated.

2. Experimental

Potassium carbonate (99.0%), sodium carbonate (99.8%) and niobium oxide (99.0%) powders were used as raw materials to synthesize $K_{0.5}Na_{0.5}NbO_3$ (KNN). The starting powders were mixed and ball milled in dehydrated alcohol for 24 h. The mixture was dried at 110 °C and calcined at 850 °C for 1 h. Lithium carbonate was added into the KNN powders to prepare tape casting slurry, with compositions of KNN–xL ($x = 0.02$, 0.04, 0.06 and 0.08). Toluene and dehydrated alcohol were mixed with a mass ratio of 2:1 to as solvent. The KNN–xL powders with a mass percentage of 55% were dispersed into the solvent and milled for 15 h. Consequently, LS bonder with a mass percentage of 15% (provided by LING-GUANG electric chemical materials Technology Corporation, Zhaoqing, China) was added into the suspensions and milled for another 3 h to obtain stable casting slurry. KNN–xL thick films were fabricated with

* Corresponding author. Tel.: +86 21 65980544; fax: +86 21 65985179.
E-mail address: apzhai@tongji.edu.cn (J. Zhai).

0925-8388/$ – see front matter © 2011 Elsevier B.V. All rights reserved.
doi:10.1016/j.jallcom.2011.04.029

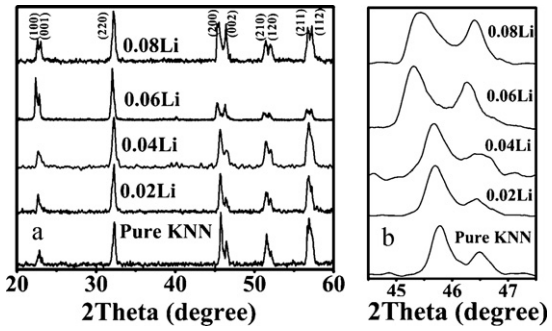

Fig. 1. XRD patterns of the KNN–*x*L thick films: (a) 20–60 °C and (b) 44.5–47.5 °C.

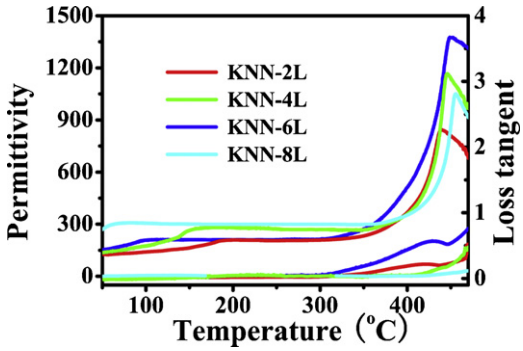

Fig. 3. Temperature dependences of dielectric constant and loss tangent of the KNN–*x*L thick films.

a conventional tape-caster with a gap of 100 μm under the blade. The green thick films were dried, cut and pressed on Al_2O_3 substrates coated with Ag–Pd bottom electrodes. The thick films were stuck on the substrates by using isostatic pressing at 200 MPa. They were annealed at 550 °C for 5 h to remove organic substances at a rate of 1 °C/min and then sintered at 1000 °C for 2 h at a heating rate of 3 °C/min.

Phase compositions of the thick films were investigated by using an X-ray diffractometer (XRD, Bruker D8 Advanced, Germany) with Cu Kα radiation. Microstructures and chemical compositions of the samples were examined by using a scanning electron microscopy (SEM, JSM EMP-800) with an EDS detector. In order to determine electrical properties of the specimens, gold electrodes with a thickness of 80 nm and a diameter of 1 mm were sputtered on surfaces of the thick films. Temperature dependences of dielectric constant and loss tangent of the thick films were measured from room temperature to 420 °C at frequencies of 1, 10, 100 and 1000 kHz by using a high-precision LCR meter (HP 4284A). Hysteresis loops and longitudinal displacement curves of the thick films were measured by using a ferroelectric test system (Precision Premier II, made in USA), connected with a miniature plane-mirror interferometer and accessory laser interferometric vibrometer (SP-S 120/500 Model, made in Germany).

3. Results and discussion

Fig. 1 shows XRD patterns of the KNN–*x*L thick films. All samples are of single phase perovskite structure. No secondary phase is detected. The orthorhombic phase is characterized by the splitting peak at $2\theta \approx 46^\circ$, where a higher peak is followed by a lower peak, whereas, the tetragonal phase exhibits a lower peak followed by a higher peak at $2\theta \approx 46^\circ$ [17,18]. Fig. 1b shows the detailed XRD patterns of the KNN–*x*L thick films over 44.5–47.5°. Pure KNN thick film is orthorhombic phase. Intensities of the two split peaks tend to be equal gradually with increasing concentration of Li, which indicates a phase transition from orthorhombic to tetragonal symmetry. This phase transition occurred at about $x = 0.06$, which suggests the coexistence of orthorhombic and tetragonal phases, i.e., the existence of a MPB, in the KNN–*x*L thick film with $x = 0.06$. Besides, a shift in diffraction peaks to lower angles with the increase of Li can also be observed. It is known that volatilization of alkali ions would happen at high temperatures which left cation vacancies and consequently made the KNN lattice shrink [19]. Li ions are supposed to occupy these vacancies at first and then enlarged the lattice which is responsible for the shift in the diffraction peaks. The limitation of Li ions in KNN lattice seems to be $x = 0.06$ according to Fig. 1b because the peaks exhibit no shift above $x = 0.06$.

Fig. 2a–e shows SEM surface images of the thick films. Grain size increases slightly with the addition of Li ions. This could be attributed to the low melting point of Li_2CO_3, which formed liquid phase that promoted sintering behaviors of the doped films. Furthermore, the addition of Li ions distorted the KNN lattice, which resulted in more defects that also could promote the grain growth of the films. The linear intercept measurement was applied to determine the average grain size of the thick film. Average grain sizes of the KNN–*x*L thick films are 1.1, 1.4, 1.5, 1.7 and 1.7 μm for $x = 0$, 0.02, 0.04, 0.06, and 0.08. However, quite a number of distinct pores are still observable in the thick films even *x* is as high as 0.08. The porous microstructures are mainly caused by volatilization of the organic substances and alkali components [20]. Chemical compositions of the thick films measured with EDS are listed in Table 1. All samples exhibit a slight fluctuation in compositions. The concentrations of K and Na are always lower than 0.5, due to their volatilization.

Fig. 3 shows temperature dependences of dielectric constant and loss tangent of the KNN–*x*L thick films. Both the O–T (orthorhomibic–tetragonal) phase-transition (T_{O-T}) and Curie point (T_C) are observed in all the KNN–*x*L thick films. T_{O-T} and T_C of KNN ceramics are 200 °C and 420 °C, respectively. T_C shifted gradually to higher temperatures as the Li content is increased. At the same

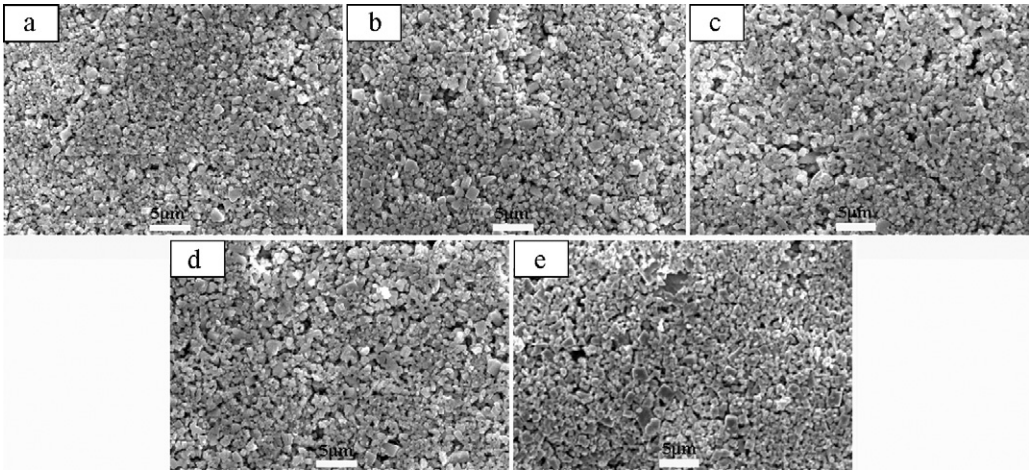

Fig. 2. SEM images of the KNN–*x*L thick films: (a) pure KNN, (b) KNN–0.02L, (c) KNN–0.04L, (d) KNN–0.06L and (e) KNN–0.08L.

Table 1
Chemical compositions of the KNN–*x*L thick films measured by EDX.

Element	K (at.%)	Na (at.%)	Nb (at.%)	O (at.%)	Formula
KNN	9.68	8.39	22.08	59.85	$K_{0.49}Na_{0.42}Nb_{1.11}O_3$
KNN–0.02L	9.26	8.69	20.82	61.23	$K_{0.46}Na_{0.42}Nb_{1.02}O_3$
KNN–0.04L	9.80	8.13	19.81	62.26	$K_{0.48}Na_{0.39}Nb_{0.95}O_3$
KNN–0.06L	8.91	8.91	22.15	60.03	$K_{0.46}Na_{0.46}Nb_{1.10}O_3$
KNN–0.08L	9.67	7.78	20.38	62.17	$K_{0.46}Na_{0.38}Nb_{0.99}O_3$

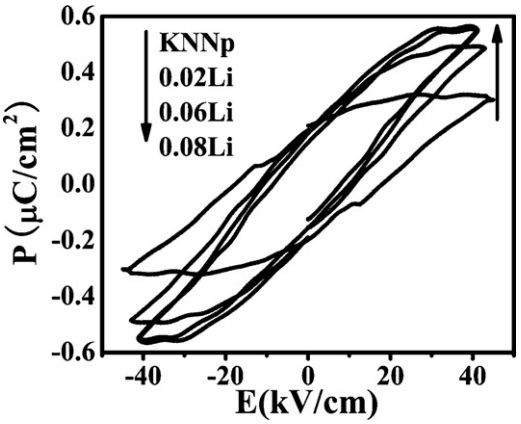

Fig. 4. *P–E* loops of the KNN–*x*L thick films.

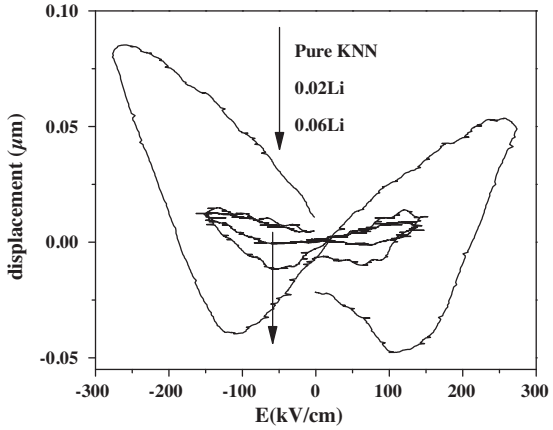

Fig. 6. Bipolar driven longitudinal strains of the KNN–*x*L thick films.

time, T_{O-T} shifted to low temperatures with increasing content of Li, indicating that the addition of Li stabilized the tetragonal phase. This result is also observed in Li doped KNN ceramics [21]. Dielectric loss tangents of the thick films are all less than 4.0% at 300 °C, which are slightly higher than that of KNN ceramics (3%) [22].

Fig. 4 shows *P–E* hysteresis loops of the KNN–*x*L thick films. Coercive fields (E_c) of the samples are illustrated in Fig. 5. E_c decreases with increasing content of Li. The presence of defects and pores caused by the volatilization of alkali components might restrict domain switching. The addition of Li not only compensated the charged defects but also improved the densification of the thick films. As a result, the domains became to more easily switchable, thus leading to a reduction in E_c. Specifically, E_c of the thick film with $x = 0.08$ is as low as 7.92 kV/cm, which is far lower than that of pure KNN and comparable with that of KNN ceramics [23]. However, an obvious hysteresis behavior is observed in these thick films. Two reasons are responsible for this kind of hysteresis behavior according to Guo et al. [24]. One is the effect of oxygen vacancy and the other is that of space charge. Both mechanisms can happen in our Li doped KNN thick films because of their porous microstructures and the volatilization of alkali components.

It has been observed in PZT thick films that substrate clamping effect introduced stresses in the films, which distorted the unit cells and thus decreased the effectiveness of polarization process. It is important to recognize the significance of the clamping effect when citing piezoelectric data [25]. Therefore, it is typical to use d_{33} values as piezoelectric constants to characterize thick-films so as to differentiate them from bulk ceramics. Here, we use dynamic d_{33} to characterize our thick films.

Fig. 6 shows longitudinal displacement curves of the samples with $x = 0$, 0.02 and 0.06. At bipolar electric field, the sample with $x = 0.06$ has the largest strain. Fig. 7 shows unipolar driven longitudinal strains of the samples with $x = 0.02$, 0.06 and 0.08. The strain values increase almost linearly and are proportional to the applied field. Longitudinal piezoelectric constants (d_{33}) were calculated from the slopes of the field-strain plots, as shown in Fig. 7. d_{33} of the thick film with $x = 0.06$ reaches a maximum value of 92 pm/V, which is much higher than the reported values of KNN thick film [6] and $0.948(K_{0.5}Na_{0.5})NbO_3$–$0.052LiSbO_3$ thick film [7]. The enhanced piezoelectric properties can be attributed to the existence of MPB.

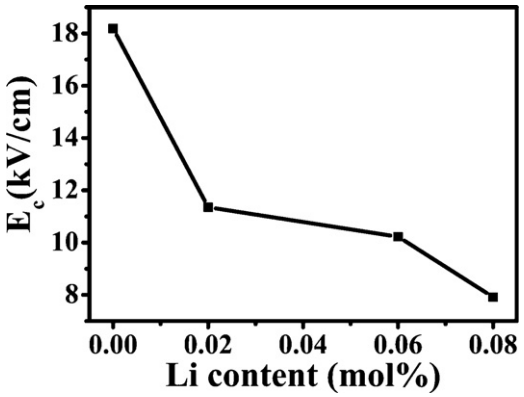

Fig. 5. E_c versus concentration of Li.

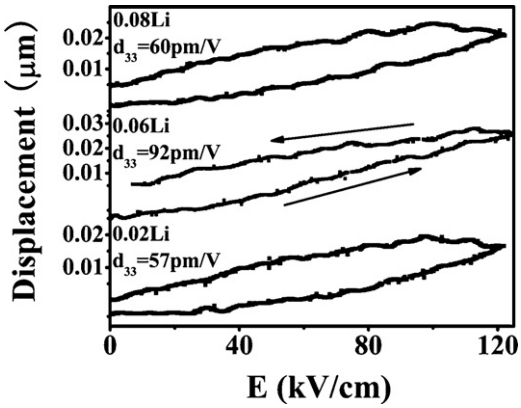

Fig. 7. Unipolar driven longitudinal strains of the KNN–*x*L thick films.

4. Conclusions

Li doped KNN thick films were fabricated by a tape casting method. A MPB was observed in the sample with Li concentration of $x = 0.06$. A very low E_c (7.92 kV/cm) was observed in the sample with $x = 0.08$. The addition of Li also decreased the values of T_{O-T} and T_C. T_C shifted to higher temperatures with increasing content of Li, whereas T_{O-T} shifted to low temperatures. Dielectric loss tangents of the doped thick films were slightly increased as compared to that of KNN ceramics. A maximized piezoelectric constant of 91.6 pm/V was observed in the sample with $x = 0.06$.

Acknowledgements

The authors would like to acknowledge the support by the National Natural Science Foundation of China under grant No. 50972108 and 50932007 and Shanghai Foundation Project under grant No. 08JC1419100. This work was also partially supported by the Research Grants Council of the Hong Kong Special Administrative Region, China (CityU No. 103307).

References

[1] H. Zhang, S. Jiang, K. Kajiyoshi, J. Alloys Compd. 495 (2010) 173.
[2] H. Ursic, M. Hrovat, D. Belavic, J. Cilensek, S. Drnovsek, J. Holc, M.S. Zarnik, M. Kosec, J. Eur. Ceram. Soc. 28 (2008) 1839.
[3] S.G. Lee, J. Alloys Compd. 454 (2008) 406.
[4] Y. Wang, J. Wu, D. Xiao, J. Zhua, P. Yua, L. Wu, X. Li, J. Alloys Compd. 462 (2008) 310.
[5] H.B. Zhang, S.L. Jiang, J. Eur. Ceram. Soc. 29 (2009) 717.
[6] L.Y. Wang, K. Yao, W. Ren, Appl. Phys. Lett. 93 (2008) 092903.
[7] J. Ryu, J.J. Choi, B.D. Hahn, D.S. Park, W.H. Yoon, Appl. Phys. Lett. 92 (2008) 012905.
[8] Y.P. Guo, K. Kakimoto, H. Ohsato, Appl. Phys. Lett. 85 (2008) 4121.
[9] Q. Zhang, B.P. Zhang, H.T. Li, P.P. Shang, J. Alloys Compd. 490 (2008) 260.
[10] F. Rubio-Marcos, M.G. Navarro-Rojero, J.J. Romero, P. Marchet, J.F. Fernández, IEEE Trans. Ultrason. Ferroelectr. Freq. Control 56 (2009) 1835.
[11] F. Rubio-Marcos, J.J. Romero, D.A. Ochoa, J.E. Garcia, R. Perez, J.F. Fernandez, J. Am. Ceram. Soc. 93 (2010) 318.
[12] Y. Saito, H. Takao, T. Tani, T. Nonoyama, K. Takatori, T. Homma, T. Nagaya, M. Nakamura, Nature 432 (2004) 84.
[13] M. Gu, L. Zhu, X. Liu, S. Huang, B. Liu, C. Ni, J. Alloys Compd. 501 (2010) 371.
[14] J. Chen, H. Fan, X. Chen, P. Fang, C. Yang, S. Qiu, J. Alloys Compd. 471 (2009) L51.
[15] A. Bardaine, P. Boy, P. Belleville, O. Acher, F. Levassort, J. Eur. Ceram. Soc. 28 (2008) 1649.
[16] Q.L. Zhao, M.S. Cao, J. Yuan, W.L. Song, R. Lu, D.W. Wang, D.Q. Zhang, J. Alloys Compd. 492 (2010) 264.
[17] M. Matsubara, T. Yamaguchi, K. Kikuta, S. Hirano, J. Jpn. Appl. Phys. 44 (2005) 6136.
[18] P. Zhao, B.P. Zhang, J.F. Li, Appl. Phys. Lett. 90 (2007) 242909.
[19] F. Rubio-Marcos, P. Ochoaa, J.F. Fernandeza, J. Eur. Ceram. Soc. 27 (2007) 4125.
[20] Y.H. Zhen, J.F. Li, J. Am. Ceram. Soc. 12 (2006) 3669.
[21] Y. Liu, Y. Huang, H. Du, H. Li, G. Zhang, J. Alloys Compd. 506 (2010) 407.
[22] Z.P. Yang, Y.F. Chang, B. Liu, L.L. Wei, Mater. Sci. Eng. A 432 (2006) 292.
[23] Y.F. Chang, Z.P. Yang, X.L. Chao, R. Zhang, X.R. Li, Mater. Lett. 61 (2007) 785.
[24] Y.Y. Guo, M.H. Qin, T. Wei, K.F. Wang, J.M. Liu, Appl. Phys. Lett. 97 (2010) 112906.
[25] R.N. Torah, S.P. Beeby, M.J. Tudor, N.M. White, J. Electroceram. 19 (2007) 95.